ISSN (O) 2321-2004, ISSN (P) 2321-5526

IJIREEICE

International Journal of Innovative Research in
Electrical, Electronics, Instrumentation and Control Engineering

Vol. 9, Issue 10, October 2021

DOI: 10.17148/IJIREEICE.2021.91020

IMPLEMENTATION OF MICRO INVERTER FOR PV SYSTEMS BASED ANFIS CONTROLLER

S. JAGADISH KUMAR

Assistant Professor, Department of Electrical and Electronics Engineering,

JNTUH College of Engineering, Jagtial, T.S., India

Abstract: The main aim of this paper is design of micro inverter for the photovoltaic scheme based adaptive neuro fuzzy inference system (ANFIS) controller. The proposed micro inverter for photovoltaic system is developed by utilizing MATLAB/SIMULINK environment. Furthermore, the control procedures are employed in accordance with the Incremental Conductance approach. The proposed system contains boost converter with incremental conductance maximum power point tracking and the H-bridge inverter with ANFIS controller. The system's reaction is observed under a variety of irradiation circumstances over time. The employed micro inverter has recompensed for changes in irradiation at the boost converter stage, and the DC/AC conversion procedure is carried out in accordance with the intended ANFIS controllers. The proposed ANFIS controller gave less THD and give higher accuracy as compared to PI Controller.

Key words: DC/DC boost converter, Micro inverter, PI, Adaptive neuro fuzzy inference system (ANFIS), Maximum power point tracking (MPPT).

I. INTRODUCTION

The energy sources can be divided into three groups one is atomic sources, fossil fuels and sustainable energy sources. The sustainable energy sources are one of the most impartment energy sources and it is commonly investigated among others. It is possible to obtain renewable energy sources (RES) from a variety of sources around the world. These include marine energies and hydropower derived from geothermal energy, biomass, solar energy, & WECS, and RES account for approximately 14 percent of global energy demand [1]. The number of renewable energy (RE) research is increasing with each passing day as a result of the depletion of fossil fuels and the conservatory impact. PV scheme are attractive increasingly popular as renewable energy sources because of their clean structure, lack of reliance on fossil fuels, long-term viability, and dependability [2].

During the day, solar cells use the sun's energy to turn light into electricity, which is then stored in batteries. 1st, 2nd, and 3rd group solar cells may be categorized. 1st-generation cells use monocrystalline and polycrystalline silicon while 2nd-generation cells are tinny solar cells. Several thin-film technologies have entered the 3rd generation of solar cells [3]. As opposed to polycrystalline cells, which is more efficient, monocrystalline cells are better. But monocrystalline cells are pricier, but as with other things, the price is based on demand. The PV system can be separated into 2 categories: grid-tied & standalone[4]. A simple PV system contains PV panels, an inverter, and a power supply circuit. Inverters are generally categorized as string inverters, micro inverters and central inverters. The 1st type inverters are central inverters as indicated in figure.1 (a) it contains strings which are included of shunt and series connected photovoltaic plants. Every string of photovoltaic panels are connected to the central inverters. Here HVDC wiring is essential for joining the central inverter that causes few drawbacks such as losses in cables in scheme. In the event of partial shading, the system might be entirely shut down [4]. The 2nd type inverters are string inverters as seen in Fig. 1.b. There is no diode loss in series with this construction, and each string has its own MPPT control. In the example depicted in Fig. 1.c, these micro inverters are linked to every photovoltaic panel, and they are associated to AC bus bar to boost system output power. PV systems with micro inverters have MPPT control applied for each PV panel. A result of this is that partial shading situations have been successfully removed [5]. In single-phase systems, micro inverters are frequently used, and this is due to several researches. For the output power of micro inverters, it is in the range of 100W to 350W, depending on the size of the PV panels. Some photovoltaic panels & therefore the issues, dust, & micro inverters are avoided, as long as PV panels are connected to the micro inverters [6]. While micro inverters do bring benefits, they also come with drawbacks such as raising the entire system cost.

ISSN (O) 2321-2004, ISSN (P) 2321-5526

IJIREEICE

International Journal of Innovative Research in
Electrical, Electronics, Instrumentation and Control Engineering

Vol. 9, Issue 10, October 2021

DOI: 10.17148/IJIREEICE.2021.91020

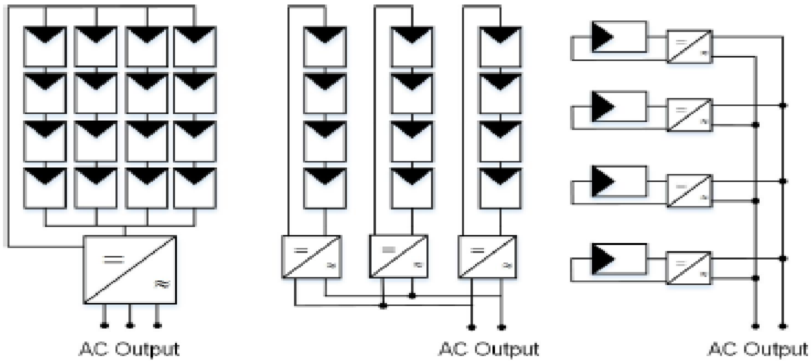

Fig1: Arrangements of photovoltaic inverter (a) Central inverters (b) String inverters (c) Micro inverters

In previous work photovoltaic scheme fed micro inverter based PI controller is researched [7] [10] but the drawback is it gives higher THDs. By overcoming this issue in this paper, photovoltaic system fed to micro inverter based FLC [11] controller is designed and comparison also studied via MATLAB/SIMULINK environment. In this paper there are two control algorithm are executed. One is incremental conductance maximum power point tracking control algorithm regulates the dc-dc boost converter and another one is ANFIS controller for controls the H-bridge inverter, it converts the dc/ac procedure. In island mode, the inverter is run without any power connection. The power voltage of the inverter is modified to 220Vrms at an output voltage of 50 Hz. The grid waveform phase tracking was not used in the present investigation.

II. PROPOSED SYSTEM

The micro inverter construction is indicated in the Fig.2. The system contains DC/DC isolated boost converter and H-bridge inverter [4]. The DC/DC boost converter is contains of switch [SB], inductor [L1], capacitor [C1] and diode [D1] wherever inverter section and converter section are isolated through HF transformer.

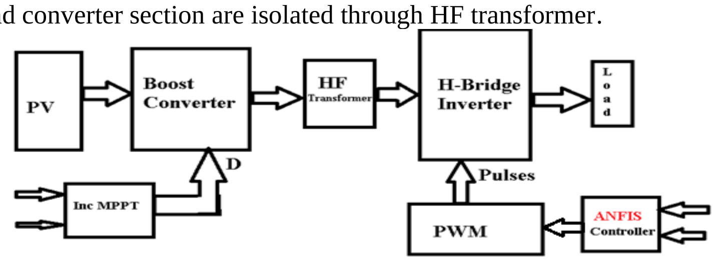

Figure.2. the construction of micro inverter

In the dc/dc boost converter the switch is MOSFET is operated via Inc MPPT. Her high frequency isolating transformer would be utilized in micro inverter scheme. The inverter (H-bridge) comprised of 4 switches namely MOSFETs are controlled through sinusoidal pulse width modulation with PI controller (in the proposed control system PI controller is ANFIS controller). In order to mitigate the current harmonics and produce the sine wave at the output of inverter the LC filter is used and it is located at the inverter output. The output and input voltages of micro inverter is supervised through the executed control software. The incremental maximum power point tracking algorithm is employed in dc/dc boost converter and for dc/ac segment of micro inverter SPWM based ANFIS control algorithm is applied. The below Table-1shows the parameters of the PV modelling panel.

Parameter	Value
Power	315 W
Voc. open circuit voltage	64.6 V
Vpm. Maximum power voltage	54.7 V
Isc Short cicuit current	61.4 V
Ipm. Maximum power current	5.76 A

Table-1 PV panel parameters

ISSN (O) 2321-2004, ISSN (P) 2321-5526

IJIREEICE

International Journal of Innovative Research in
Electrical, Electronics, Instrumentation and Control Engineering

Vol. 9, Issue 10, October 2021

DOI: 10.17148/IJIREEICE.2021.91020

III. DESIGN OF MICRO INVERTER

A) DC/DC boost converter

The dc/dc boost converter also called as step up converter. It converts lower input dc voltage into higher dc voltage. The input energy will be momentarily stored and released as a greater voltage in the output. This is done in inducers or condensers [8]. The condenser is used to minimize the voltage waveform oscillation. A switching device with switching pulse generated through maximum power point tracking controller is utilized to minimize the power switching losses. Fig. 3 indicates the illustration of dc/dc boost converter wherever the proposal constraints are assumed follows;

$$V_{out} = \frac{V_{in}}{1-D} \qquad (1)$$

$$C \geq= \frac{I_o.D.T_s}{\Delta V_{max}} \qquad (2)$$

$$L \geq= \frac{V_{in}.D}{\Delta I.f_s} \qquad (3)$$

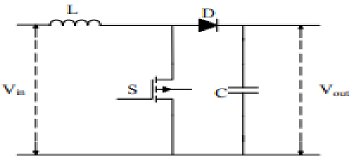

Figure.3. Arrangement of the dc/dc boost converter

The dc/dc boost converter operates in two modes. One is charging mode and second one is discharging mode of L and C constituents.

The switch is in the “ON” position and the inductor is charging to its maximum capacity in the 1st mode. After that, the switch is set to the “OFF” position and the inductor discharges through the output to deliver power to the load. Fig-4 and Fig-5 indicates the various operating modes.

1) 1st mode of operation (0<t<toff)

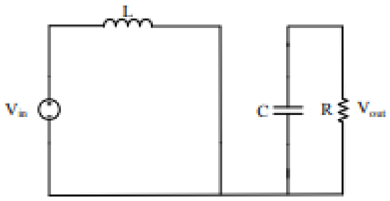

Figure 4 boost converter scheme when the switch is "ON"

2) 2nd mode of operation (toff <t<Ts)

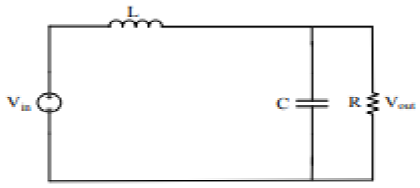

Figure.5 boost converter scheme when the switch is "OFF"

When the inductor's loading current is less than the output current, the converter's output will not be boosted. The values presented in Table-2 represent the computed DC/DC boost converter.

Parameter	Value
C, Capacitor	53 µF
L, Inductor	520 µH
Fsw , Switching Frequency	20 KHz
Vin ,Input voltage of boost converter	54 V
V, Vdc link , output voltage of boost converter	311 V

Table-2. Boost Converter Parameters

B)Maximum Power Point Tracking Control Algorithm

In this paper incremental conductance MPPT is used for controlling the boost converter. It so complex and ensures good control under different situations in the atmosphere. This illustration, figure 7, illustrates the flowchart of the incremental conductance MPPT in accordance with the first flowchart which first uses voltage and current measurements from the PV panel to gauge the incremental conductance. These sensors obtain current and voltage. At the maximum power point, the slope of the PV array is zero. When the slope is negative, it signifies the tracing point is located one positive power position to the right of the maximum power point. Else slope is positive slope the tracing point is left the maximum power point.

ISSN (O) 2321-2004, ISSN (P) 2321-5526

IJIREEICE

International Journal of Innovative Research in
Electrical, Electronics, Instrumentation and Control Engineering

Vol. 9, Issue 10, October 2021

DOI: 10.17148/IJIREEICE.2021.91020

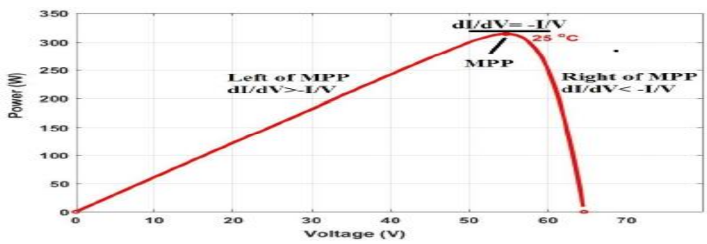

Figure.6 The concept behind the incremental conductance technique on a P–V plot of a photovoltaic panel

These initial equations are listed below.

$P = V.I$ (4)

$$\frac{dP}{dV} = I + V\frac{dI}{dV} \quad (5)$$

$$\frac{dP}{dV} = I + V\frac{dI}{dV} = 0 \quad (6)$$

$$\frac{dI}{dV} = -\frac{I}{V}\left(\frac{dP}{dV} = 0\right) \quad (7)$$

$$\frac{dI}{dV} > -\frac{I}{V}\left(\frac{dP}{dV} > 0\right) \quad (8)$$

$$\frac{dI}{dV} < -\frac{I}{V}\left(\frac{dP}{dV} < 0\right) \quad (9)$$

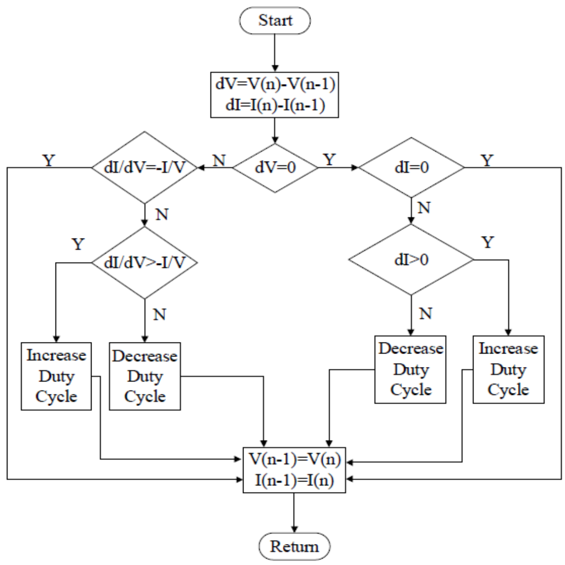

Figure7. Flow chart of incremental conductance MPPT algorithm

C) H-Bridge Inverter with SPWM technique

The H-bridge inverter which converts direct current to alternating current. The periodic waveform is the output voltage of the inverter, which in non-sinusoidal. The figure.8 indicates the H-bridge inverter topology.

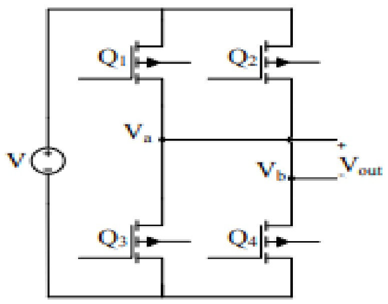

Figure.8 Inverter circuit

The positions of switches are indicated in Table-3. Here four various switching positions to producing the output voltage.

Situations	Conducting switching	Va	Vb	Vout
1	Q1 and Q4	V/2	-V/2	V
2	Q2 and Q3	-V/2	V/2	-V
3	Q1 and Q3	V/2	V/2	0
4	Q2 and Q4	-V/2	-V/2	0

Table-3. H-bridge inverter switching states

By seeing the table, the 1st and 2nd positions are utilized to produce the AC voltage. These states are obtained via PWM technique. The pulse width modulation techniques are different types namely sinusoidal PWM., Space Vector PWM and discontinues space vector PWM. The sinusoidal pulse width modulation technique is generally utilized as a

ISSN (O) 2321-2004, ISSN (P) 2321-5526

IJIREEICE

International Journal of Innovative Research in
Electrical, Electronics, Instrumentation and Control Engineering

Vol. 9, Issue 10, October 2021

DOI: 10.17148/IJIREEICE.2021.91020

switching technique i.e., it acquired via comparing the triangular wave and sinusoidal waveform as reference wave. Inverter switching frequency is determined by the triangular waveform. The reference waveform's frequency is critically crucial because it sets the inverter output voltage. In Fig.-9, we see the switch's duty ratio is adjusted using a sinusoidal reference waveform.

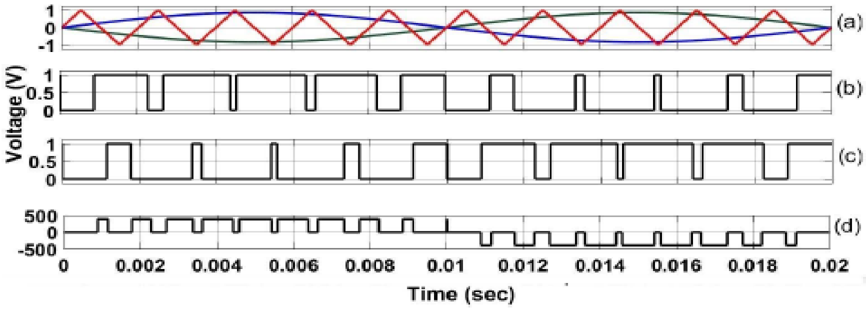

Figure-9 Generation of SPWM (a) Comparison of reference sinusoidal waveform and triangular waveform (b) switching pulses of Q4 and Q1(c) switching pulses of Q3 and Q2 (d) waveform of output voltage

SPWM WITH ANFIS CONTROLLER

In the SWPM controller the PI controller replaced by adaptive neuro fuzzy inference system (ANFIS) controller for reduction of harmonics in the grid voltage. The figure.10 indicates the generation of sinusoidal pulse width modulation switching pulses with ANFIS controller. The output voltage (feedback signals) is compared with the reference voltage. And this signal given to the ANFIS controller after that it is product with the sin signals. This sin signals is compared with the triangular wave and produces the pulses. The ANFIS controller gives less THD compared to conventional PI controller.

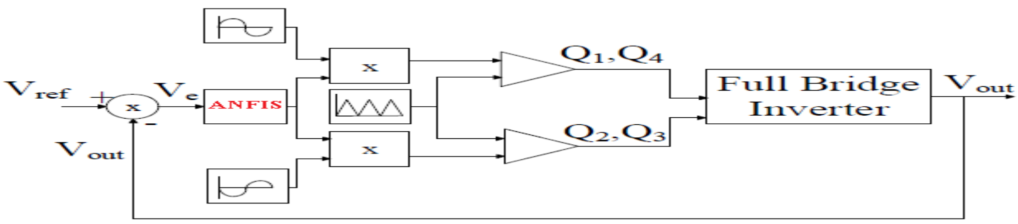

Fig. 10 Generation of sinusoidal pulse width modulation switching pulses with ANFIS controller

IV. PROPOSED CONTROLLER

ANFIS CONTROLLER

The ANFIS stands for Adaptive neuro fuzzy inference system. ANFIS controller is the grouping of fuzzy logic and neural network. Depending on the inputs of the neural network, several inputs are transmitted through the neural network. Neural network is trained according to the performance and inputs. The performance is added to the fuzzy logic after training the neural network. The rules (IF and THEN) and (MF) membership functions are generated by Fuzzy logic. The below Figure-11 shows the ANFIS architecture.

ISSN (O) 2321-2004, ISSN (P) 2321-5526

IJIREEICE

International Journal of Innovative Research in
Electrical, Electronics, Instrumentation and Control Engineering

Vol. 9, Issue 10, October 2021

DOI: 10.17148/IJIREEICE.2021.91020

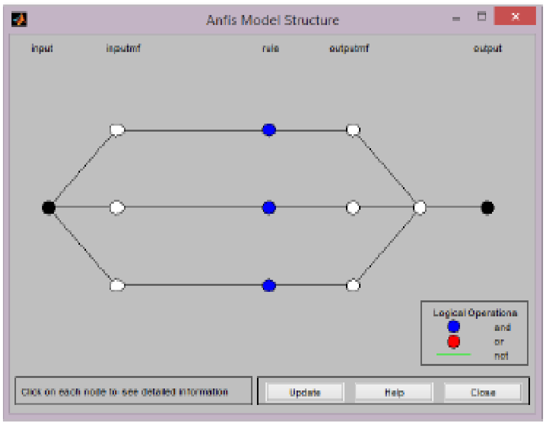

Fig. 11. ANFIS architecture

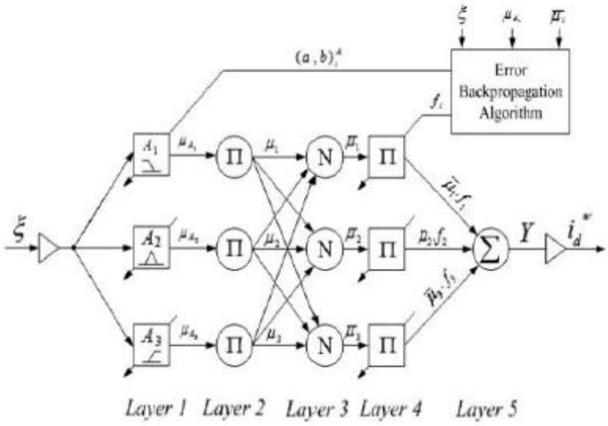

Fig.12 Schematic of the proposed ANFIS

Neuro Fuzzy controller will be error between reference voltage of dc-link and the exact dc-link voltage (ξ = Vdc*-Vdc), and the precondition and the following parameters will also be set by a similar error. The dc-link voltage controller provides the active current (id *') section that is further adapted to calculate the active current injected into RES (iRen).

Layer 1: This is a layer of fuzzification. Membership degrees for each input variable are determined in this layer. ANFIS input variables are selected as error (e) and error change (Δe). In order to reduce the error of measurement as shown in Figure-12, trapezoidal and triangular registration abilities.as described below the node conditions are,

$$O_i^1 = \mu_{Ai}(x) = \frac{1}{1+\left[\left(\frac{x-c_i}{a_i}\right)^2\right]^{bi}} \qquad (10)$$

Where x is the node-i entry, Ai is the linguistic variable associated with it, and {ai, bi, ci} is the premise parameter set.

Layer 2: This layer is the inferior layer of the rule. Each node in this layer is a fixed node labelled as a ∏ the input node multiplies and the product sends out. Each node output is the firing strength of a fuzzy rule.

$$O_i^2 = \mu_i = \mu(x)\mu(y) \qquad i = 1,2,3 \qquad (11)$$

Layer 3: It is the normalization layer. Each layer node is an N-labeled circle node. The i-th node computes the ratio of the firing force of the rule's to the amount of the firing force of all rule's.

$$O_i^3 = \overline{\mu_i} = \frac{\mu_i}{\mu_1+\mu_2+\mu_3} \qquad i = 1,2,3 \qquad (12)$$

Layer 4: It is the resulting layer. All nodes have network functionality and adaptive mode

$$O_i^4 = \overline{\mu_i}.f_i = \overline{\mu_1}\left(a_0^i + a_1^i\epsilon\right) \qquad i = 1,2,3 \qquad (13)$$

The resulting parameter set where the output of Layer 3 is wi (a0, a1).

Layer 5: It is the output layer. The only node within this layer is a fixed node labelled as ∑ a combination of all incoming signals that calculates the total output.

$$O_i^5 = \mu_i = \sum_i \overline{\mu_i}\, f_i \qquad i = 1,2,3 \qquad (14)$$

The ANFIS parameters are modified with the following back propagation error:

$$\frac{\partial E}{\partial O^5} = k_1.e + k_2.\Delta e \qquad (15)$$

Signals error (e) and the change of error (Δe) multiplied by the k1 and k2 coefficients.

$$\alpha_{k+1} = \alpha_k - n\frac{\partial E}{\partial \alpha_k} \qquad (16)$$

Vol. 9, Issue 10, October 2021
DOI: 10.17148/IJIREEICE.2021.91020

Where α is one ANFIS parameter and the study rate is η. The next training iteration will be reduced by the error.

V.SIMULATION RESULTS

EXISTING PI CONTROLLER

The Fig.13 shows the system block diagram with PI controllers which contains the PV array, boost converter and H-bridge inverter. Fig.14 indicates the PV voltage and current under the various irradiance conditions. Fig.15 indicates the output voltage of the boost converter, Fig.16 indicates the output voltage and current of the load and fig.17 indicates the THD% output voltage and current of the load.

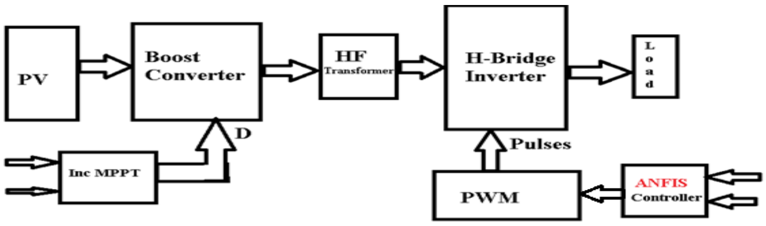

Figure.13 Proposed system block diagram with PI controller

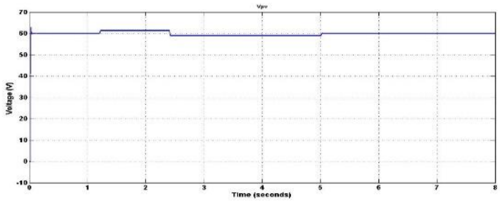

(a)

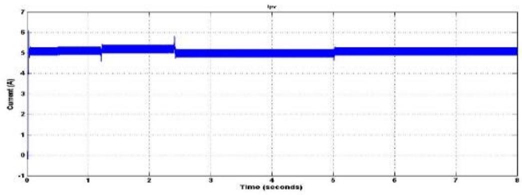

(b)

Figure .14 Under several irradiation conditions (a) Vpv and (b) Ipv

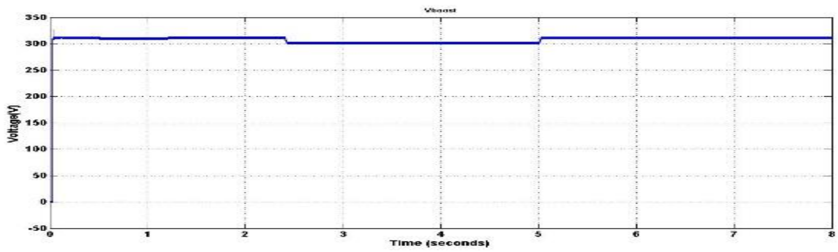

Figure.15 Boost converter output voltage

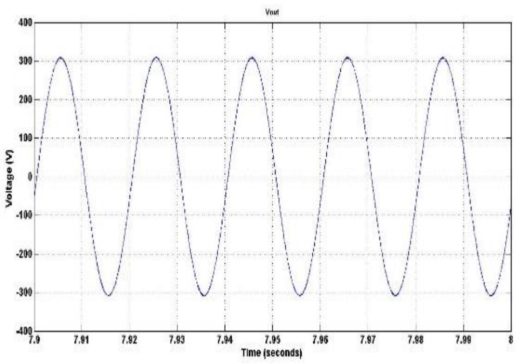

(a)

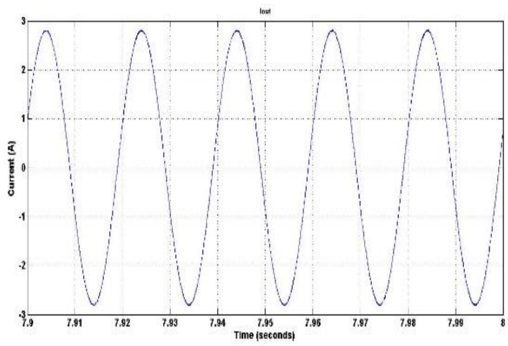

(b)

Figure.16 (a) Output voltage & (b) Output current of Load

IJIREEICE

ISSN (O) 2321-2004, ISSN (P) 2321-5526

International Journal of Innovative Research in
Electrical, Electronics, Instrumentation and Control Engineering

Vol. 9, Issue 10, October 2021

DOI: 10.17148/IJIREEICE.2021.91020

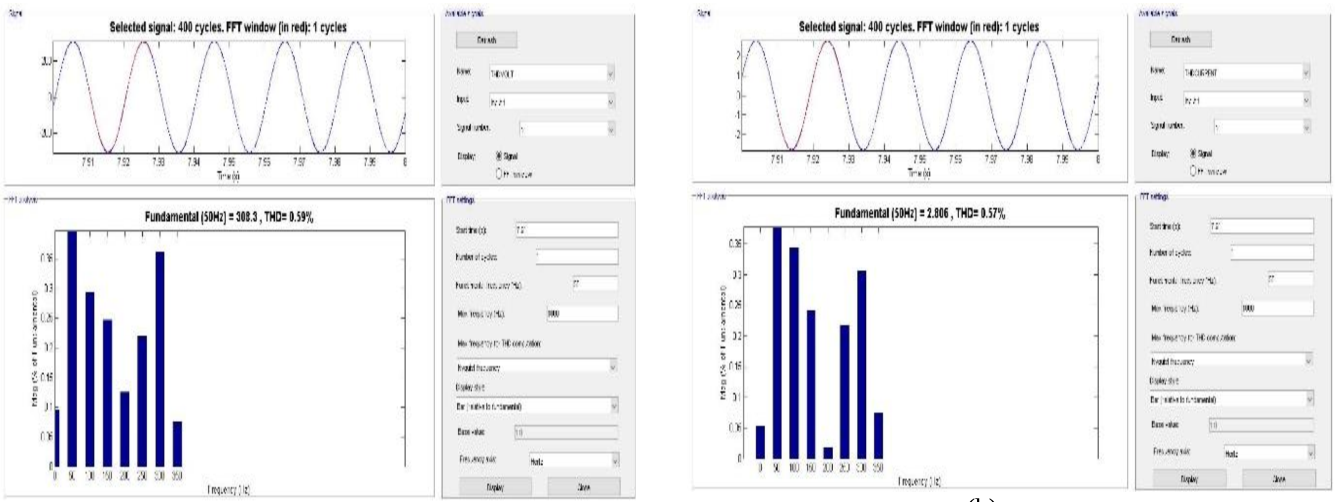

(a) (b)

Figure.17 (a) THD% Output voltage is (0.59%) (b) THD% of Output current is (0.57%)

PROPOSED SYSTEM WITH ANFIS CONTROLLER

The Fig.18 shows the system block diagram with ANFIS controller which contains the PV array, boost converter and H-bridge inverter. Fig.19 indicates the output voltage and current of the load and fig.20 indicates the THD% output voltage and current of the load. By observing three controller the ANFIS gives less THD as shown in Table-4.

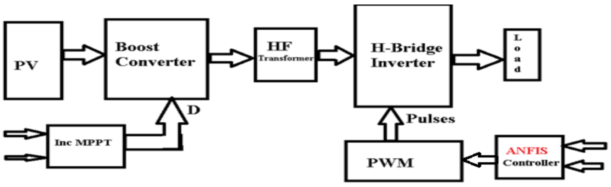

Fig.18 Proposed system block diagram with ANFIS controller

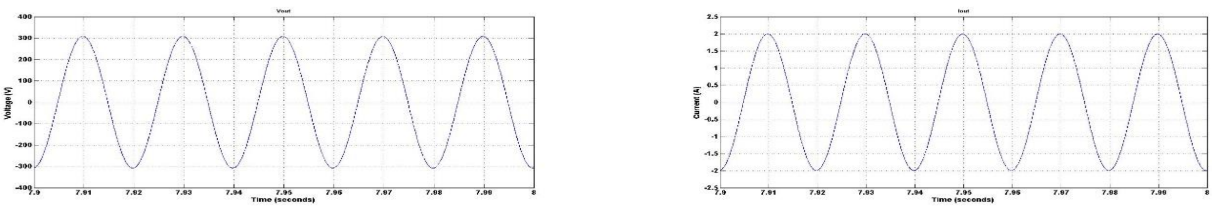

(a) (b)

Figure.19 (a) Output voltage & (b) Output current of Load

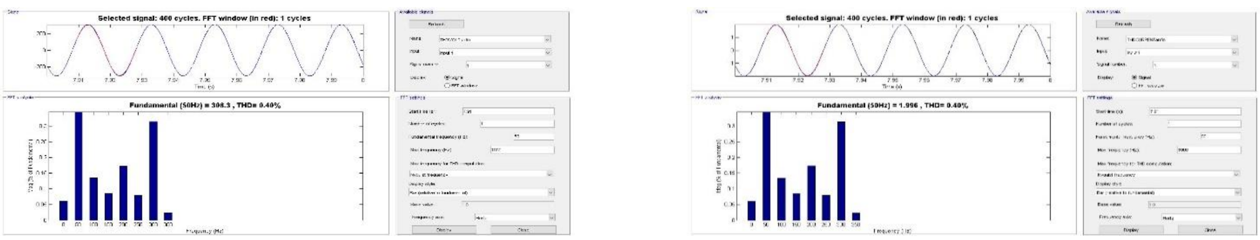

(a) (b)

Figure.20 (a) THD% Output voltage is (0.40%), (b) THD% of Output current is (0.40%)

ISSN (O) 2321-2004, ISSN (P) 2321-5526

IJIREEICE

International Journal of Innovative Research in
Electrical, Electronics, Instrumentation and Control Engineering

Vol. 9, Issue 10, October 2021

DOI: 10.17148/IJIREEICE.2021.91020

TABLE-4 COMPARISION TABLE

THD	Pi Controller	Fuzzy Controller	ANFIS Controller
THD % of grid voltage	0.59%	0.44%	0.40%
THD % of grid current	0.57%	0.44%	0.40%

CONCLUSION

This paper suggests the design of a micro inverter for PV systems based adaptive neuro fuzzy inference system (ANFIS) controller. In this system the dc voltage of PV array have been changed in to ac voltage at the micro inverter output. In spite of decreasing and increasing solar irradiance, the inverter output voltage does not change and it is attained as pure sine wave. The harmonic analysis approve that the suggested inverter is able to produce the conversion of the power at the necessary power quality and power rate. ANFIS controller give less THD values of current and voltage compared to conventional pi controller.

REFERENCES

[1] E. Kabalci, A. Gorgun, " Design and implementation of a PI-MPPT based buck-boost converter", ECAI 2015 - Bucharest, ROMÂNIA, pp. 23-28.

[2] N.L. Panwara, S.C. Kaushikb, S. Kotharia, "Role of renewable energy sources in environmental protection: A review", Ren.Sus. En. Rew vol. 15, 2011, pp. 1513–1524.

[3] O. P. Mahela, A. G. Shaik, "Comprehensive overview of grid interfaced solar photovoltaic systems", ", Ren.Sus. En. Rew vol. 68, February 2017, pp. 316-332.

[4] A. M. Bagher, M. M. A. Vahid, M. Mohsen, "Types of Solar Cells and Application", American Journal of Optics and Photonics, 21 August 2015, pp. 94-113.

[5] R. Dhivya, K. Jaiganesh, Dr. K. Duraiswamy, "MATLAB simulation of photovoltaic micro inverter system using MPPT algorithm", Int.J. Sci. En. Res. vol. 4, December2013, pp. 2077-2082.

[6] J. L. Diaz-Bernabe, A. Morales-Acevedo, "Simulation of a double-stage micro-inverter for grid-connected photovoltaic modules", in 2016 Electrical Engineering, Com (CCE), Mexico ,September 26-30 2016. [7] SunPower Pv Panel http://www.solar-facts-and-advice.com/supportfiles/sp_315ewh_en_ltr_p_ds.pdf [14.05.2017]

[8] N. Prabaharan, K. Palanisamy, "Analysis and integration of multilevel inverter configuration with boost converters in a photovoltaic system", EnConMan vol. 128, 15 2016, pp. 327–342.